CrossMark

Effect of Particle Mixture on Seepage Properties of Crushed Mudstones

Dan Ma · Haibo Bai · Zhanqing Chen · Hai Pu

Abstract Crushed rocks, especially mudstones, whose seepage properties are strongly influenced by particle mixture during compaction due to muds will be washed away after water flow. The present study focuses on the porosity evolution, particle crushing and non-Darcy seepage properties, during the compaction, of a crushed mudstone particle size mixture. An experiment based on a self-designed water flow apparatus, the MTS 815.02 system and a non-Darcy testing method were performed to investigate the effect of particle size mixture on seepage properties and compaction behavior of crushed mudstones. In particular, the Reynolds number calculation of particle mixture shows that water flow has involved the influence of non-Darcy flow. Testing results indicate that: (1) The porosity of crushed mudstones is strongly influenced by compaction (axial displacement) and particle mixture. The porosity decreases with the increase in axial displacement and decrease in bigger particle size, respectively. (2) During the compaction, some larger particles were crushed which is a main reason to cause size 0–2.5 mm. Muds washed away are the main reason for weight lost in mudstone samples due to the effect of water seepage. (3) Non-Darcy seepage properties of crushed mudstones were strongly influenced by mixture sizes and compaction, and in general, during the axial compression, the permeability k decreases while the non-Darcy coefficient β increases with the decrease in porosity ϕ. (4) The fluctuations of k–ϕ and β–ϕ curves show that the lager the particle size, the more the fluctuation displayed in the curves. The permeability k of minimum size shows one order of magnitude less than that for largest one. (5) The porosity, particle crushing and seepage properties of crushed mudstones are not only related to compaction levels, mixture sizes, but also related to the style of arrangement.

Keywords Crushed particle mixture · Mudstone particle · Non-Darcy flow · Compaction · Experimental investigation

D. Ma · H. Bai (✉) · Z. Chen · H. Pu
State Key Laboratory for Geomechanics and Deep Underground Engineering, China University of Mining and Technology, Xuzhou 221116, Jiangsu, China
e-mail: hbbaicumt@126.com

 Springer

List of symbols

d	Average diameter of the grains (L)
d_p	Diameter of piston (L)
d_r	Diameter of mudstone sample (L)
h_0	Initial height of the crushed mudstone sample (L)
H_1	Cylinder tube height (L)
H_2	Piston height (L)
H_3	Thickness of the felt filtration pad (L)
H_4	Thickness of porous plate (L)
i, n	Spatial indices $(-)$
k	Permeability (L^2)
L	Sample length (L)
m	Mass of the crushed mudstone sample (M)
p	Pore pressure $(ML^{-1}T^{-2})$
p_a	Pore pressure connected with atmosphere $(ML^{-1}T^{-2})$
p_b	Pore pressure at the intake boundary $(ML^{-1}T^{-2})$
Q	Cross section area of the cylinder tube (L^2)
Re	Reynolds number $(-)$
S	Axial displacement (L)
t	Time (T)
v	Water flow velocity (LT^{-1})
v_p	Supercharger piston velocity (LT^{-1})
z	Vertical axis going through the center of the sample (L)
∂	Partial differential operator $(-)$
$\partial()/\partial z$	Nabla operator (L^{-1})
β	Non-Darcy coefficient (L^{-1})
μ	Kinetic viscosity $(ML^{-1}T^{-1})$
ϕ	Porosity $(-)$
ρ_s	Mass density (ML^{-3})
ρ_w	Water density (ML^{-3})

1 Introduction

In longwall mining, the overburden strata of a coal seam are disturbed and typically form four zones of disturbances, as shown in Fig. 1, in response to the mining (Peng 2006). Equilibrium can be developed in the disturbed overburden, with the consolidation of the caved zone after mining operations (Pappas and Mark 1993). In such cases, besides the factors such as the geological conditions, groundwater and extraction percentage of underground mines (Singh 1992; Blodgett and Kuipers 2002; Miao et al. 2011; Bai et al. 2013; Ma et al. 2015), it is important to take into account the seepage flow characteristics (Shi et al. 2014) of the crushed rocks in caved zones under constant loadings of overburden strata (Ding et al. 2014), because the study of seepage properties of crushed rocks plays an important role in coal mining engineering as it helps in understanding the problems well. After re-compaction, the crushed mixture soft rocks in caved zones have water-resisting property if the internal crack closing (Rong and Bai 2014), generally refer to mudstone, a type of mudrock, is a fine grained sedimentary rock whose original constituents were clays or mud.
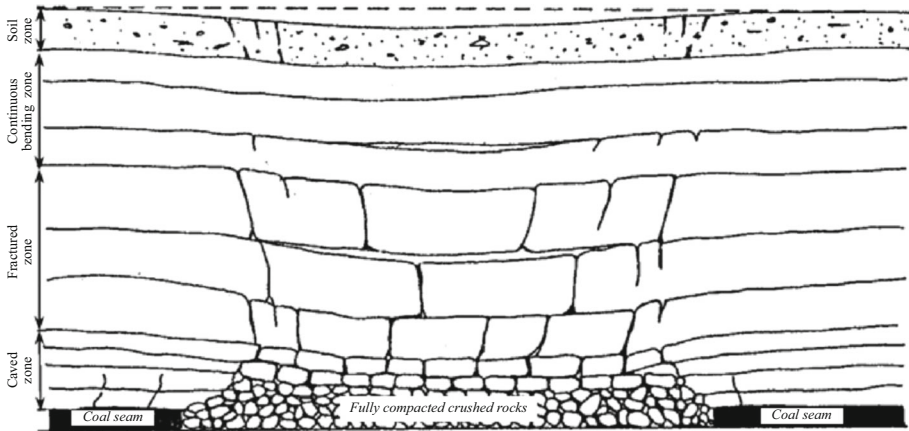
Fig. 1 Four zones of overburden strata above a longwall panel (Peng 2006)

Interbedded mudstone strata are widely distributed around the world, and also in Xiaojihan Coal Mine, Northern Shaanxi of China. The interbedded deposit of mudstone in Xiaojihan Coal Mine was mainly formed in Upper Triassic, Lower and Upper Jurassic periods (XGMRE, 2009). The interbedded deposit formed in Upper Triassic period includes the Wayaobao formation with 620–740 m in thickness, and the Yongping formation with 740–880 m. The thickness of the interbedded deposit formed in Lower Jurassic period, which is called as the Fuxian formation, is about 560–630 m. That formed in Upper Jurassic period includes the Anding formation with 90–200 m, the Zhiluo formation with 200–320 m, and the Yan'an formation with 320–560 m in thickness. The general geologic stratigraphy in the Xiaojihan Coal Mine area is summarized in Fig. 2, the coal seam 2 is at a depth of 318–382 m, with an average thickness of 2.7 m and dip angle of $0°–1°$, both the roof and floor of coal seam 2 are mudstone, which can be accessed into caved zones (goaf) easily after mining.

Seepage properties of crushed rocks after compaction play an important role in coal mining engineering; therefore, the evaluation on the compaction quality of the mixture is very important. Many factors, such as particle shape, soil type and compaction effort, may affect the compaction quality of soils (Hamdani 1983; Blotz et al. 1998; Cho et al. 2006). Many other behaviors of particles, such as permeability (Yan et al. 2010; Wang et al. 2012, 2013a; Miao et al. 2011), compressive deformation (Wang et al. 2013d), angle of repose (Wang et al. 2013b), shear strength (Fredlund et al. 1978; Wang et al. 2013c) and even fracture behavior (Wang et al. 2007; Ma et al. 2013), may also be affected by soil density mixture. The soil particles may be crushed during the loading (Hardin 1985; Lade et al. 1996; Coop et al. 2004; Lobo-Guerrero and Vallejo 2005; Casini and Viggiani 2011); many factors may cause the particle crushing during the loading, such as the applied stress, the initial grading of the tested soil (Coop et al. 2004) or that of the artificial crushable material (Casini et al. 2013), the change in particle mixture (Jamei et al. 2011), the complex shape in physics and geometry (Wu et al. 2009) and the geological framework (Aydin et al. 2006).

The particle rearrangements due to seepage forces, with the formation of channels and compacted regions of granular medium, have been analyzed (Johnsen et al. 2007, 2008; Niebling et al. 2012), while the impact of water seepage in crushed rock cannot be ignored. In order to monitor water seepage flow in crushed (broken) mudstones and other rock masses, the seepage properties have been tested by many experimental methods (Kogure 1976; Zoback and Byerlee 1976; Pradip and Venkataraman 1995; Legrand 2002; Engelhardt and Finsterle
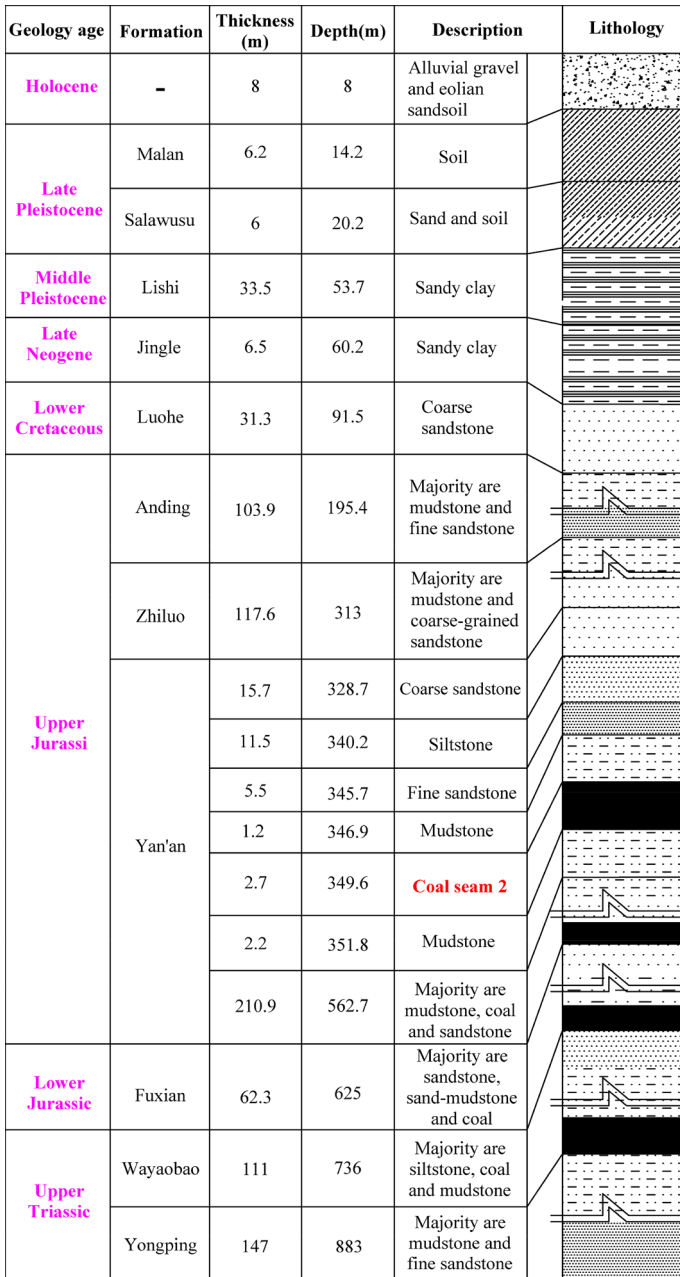
Geology age	Formation	Thickness (m)	Depth(m)	Description	Lithology
Holocene	-	8	8	Alluvial gravel and eolian sandsoil	
Late Pleistocene	Malan	6.2	14.2	Soil	
	Salawusu	6	20.2	Sand and soil	
Middle Pleistocene	Lishi	33.5	53.7	Sandy clay	
Late Neogene	Jingle	6.5	60.2	Sandy clay	
Lower Cretaceous	Luohe	31.3	91.5	Coarse sandstone	
Upper Jurassi	Anding	103.9	195.4	Majority are mudstone and fine sandstone	
	Zhiluo	117.6	313	Majority are mudstone and coarse-grained sandstone	
	Yan'an	15.7	328.7	Coarse sandstone	
		11.5	340.2	Siltstone	
		5.5	345.7	Fine sandstone	
		1.2	346.9	Mudstone	
		2.7	349.6	Coal seam 2	
		2.2	351.8	Mudstone	
		210.9	562.7	Majority are mudstone, coal and sandstone	
Lower Jurassic	Fuxian	62.3	625	Majority are sandstone, sand-mudstone and coal	
Upper Triassic	Wayaobao	111	736	Majority are siltstone, coal and mudstone	
	Yongping	147	883	Majority are mudstone and fine sandstone	

Fig. 2 General geologic stratigraphy Xiaojihan Coal Mine

2003; Miao et al. 2004, 2011). The seepage properties of crushed rock masses were tested, and a water flow apparatus for crushed stone, justified its feasibility, were designed (Liu et al. 2003). The rules in the variation of compaction, expansion and seepage characteristics of natural and saturated crushed rocks and discovered a logarithmic relationship between the

permeability coefficients and axial pressures were studied (Ma 2003). The flow properties of a non-Darcy flow in crushed rocks were obtained, and it appears that the water seepage in crushed rocks no longer obeys the Darcy law, but the Forchheimer equation. The characteristics of a non-Darcy flow are even more remarkable when the rock is under a less porous ratio (Li et al. 2005; Miao et al. 2011). A nonlinear dynamic model of the fluid–structure interaction for non-Darcy seepage in a crushed rock mass was established based on the principle of effective stress in porous media. The result shows that when the parameter of a nonlinear term increases or the system is far from a steady state, the system will gradually lose stability, resulting in dynamic disasters of water seepage (Huang et al. 2005). Based on the steady-state seepage method, Liu et al. (2012) used the MTS815.02 and a self-designed seepage instrument for over-broken stone to measure seepage properties of water flows in three types of crushed rock samples. Recently, Ma et al. (2014) conducted an experimental investigation on permeability measurement of water flow in crushed rocks, however, they did not take the particle size as mixture in the study. So far, the non-Darcy flow seepage properties rules of crushed mudstones to variable particle mixture under compaction are still not provided.

Driven by importance of non-Darcy seepage properties of water flow in crushed mudstones under variable particle mixture during compaction, this study further develops a method which includes the non-Darcy condition of measuring, calculating and quantifying the influence of varying particle size and axial displacement on water seepage properties of crushed mudstones. This paper first presents the test specimens of crushed mudstone, a self-designed water flow apparatus which can be connected to the electrohydraulic servo-controlled test system MTS815.02 (MTS System Corporation 1993) in Sect. 2. Section 3 introduces the detailed testing method and procedure. A non-Darcy equation (approach) and the relationships between non-Darcy seepage properties and variable particle mixture during compaction are given in Sect. 4. Experimental study on crushed mudstones and the discussion to the testing data are given in Sect. 5. Finally, Sect. 6 concludes and discusses the implication of these findings.

2 Tested Mudstone Material and Equipment

2.1 Mudstone Material and Specimen Preparation

The mudstone specimens used in the seepage properties test were taken from about -350 m strata, as shown in Fig. 2, both roof and floor for coal seam 2 in Xiaojihan Coal Mine in Shaanxi province of P.R. China and were prepared in the laboratory.

The mudstones are crushed into particles with different sizes less than 20 mm for the purpose of preparing the tested materials. The procedure to crush the rock blocks includes two steps. Firstly, the mudstone blocks are artificially crushed into particles less than 60 mm in diameter using iron hammers and steel piercers. Then, the artificially crushed particles are mechanically crushed again into particles less than 20 mm in size by a special rock breaker.

The crushed mudstone particles are, respectively, separated into four groups based on the particle sizes 2.5–5, 5–10, 10–15 and 15–20 mm using a high-frequency vibration screening test sieve machine (Fig. 3). The five samples are constituted by particle sizes 2.5–5, 5–10, 10–15 and 15–20 mm as weight ratio 1:1:1:1, 3:1:1:1, 1:3:1:1, 1:1:3:1 and 1:1:1:3, respectively, and the weight to each sample with 1800 g. The particle groups of mudstone are, respectively, mixed according to the grain size distribution shown in Table 1. Figure 4 shows the prepared crushed mudstone separated by the screening test sieve machine.

Fig. 3 A high-frequency
vibration screening test sieve
machine

Table 1 Mudstone particle size distribution to each group sample

No.	Total mass (g)	Weight ratio to each particle size	Weight to each particle size (g)			
			2.5–5 mm	5–10 mm	10–15 mm	15–20 mm
1	1800	1:1:1:1	450	450	450	450
2	1800	3:1:1:1	900	300	300	300
3	1800	1:3:1:1	300	900	300	300
4	1800	1:1:3:1	300	300	900	300
5	1800	1:1:1:3	300	300	300	900

2.2 Testing Equipment

The MTS815.02 system and a self-made water flow apparatus are the two major components in the testing system, as shown in Fig. 5, and Fig. 6 illustrates the system connection and principle. The loading platen (*1*) is used to offer the axial loading pressure. The porous plate (*4*) and (*14*) can ensure that the fluid flows evenly, and the felt filtration pad (*5*) and (*15*) can prevent the system from being polluted by the fluid. The rock specimen (*16*) and the cylinder tube (*7*) are separated by the epoxy resin layer (*6*), which can prevent the radial flow of fluid. The cylinder tube and the three-axis room base of the system are connected by the one-way
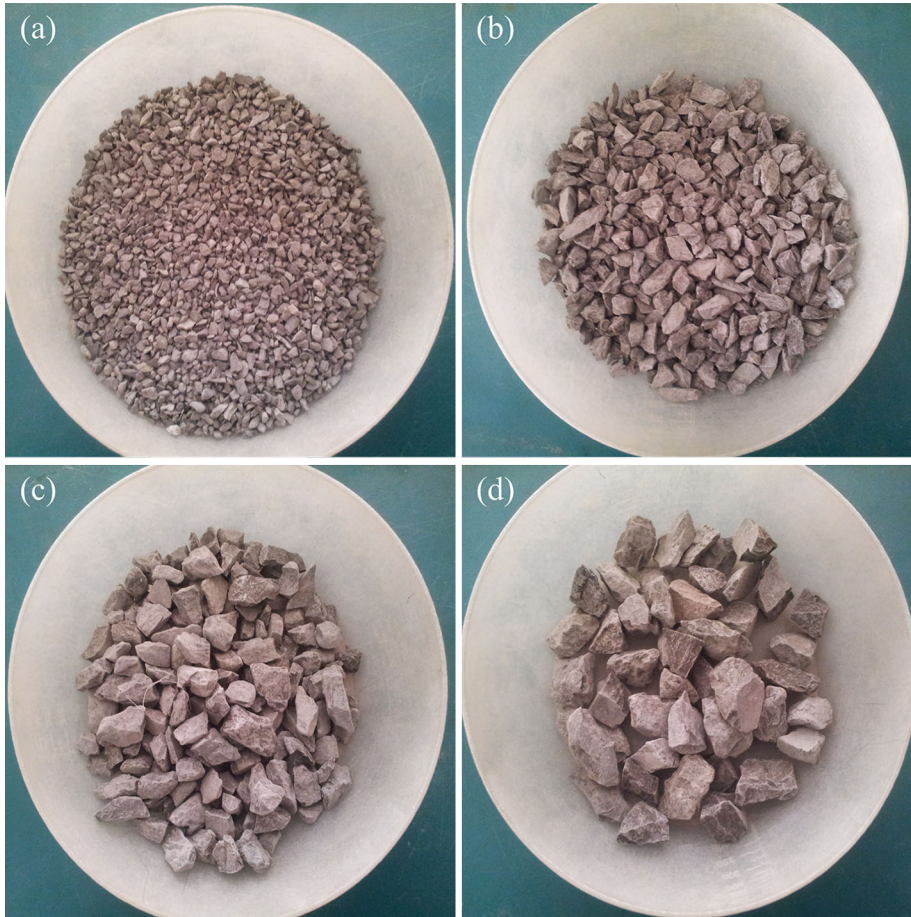
Fig. 4 Crushed mudstone separated by the screening test sieve machine. Particle size: **a** 2.5–5 mm, **b** 5–10 mm, **c** 10–15 mm and **d** 15–20 mm

valve, which includes the mechanical bolt (*9*), mechanical spring (*10*), valve core (*11*), valve chest (*12*) and base plate (*13*). The O-shaped rubber seal rings (*2*) and (*8*) are, respectively, used to enclose the axial gaps between the spherical indenter of the axial load system and the piston (*3*), the cylinder tube and valve chest.

The MTS815.02 system has been previously used in research that investigated the seepage properties of fractured rocks (Chen et al. 2004; Ma et al. 2013) and different type-crushed rocks (Miao et al. 2011; Liu et al. 2012; Ma et al. 2014); however, the tests did not consider the impact of particle mixture on seepage properties for crushed mudstones.

3 Testing Method and Procedure

Crushed mudstone samples needed to be completely saturated by water before each experiment and at the beginning of seepage, they must be saturated again under low axial pressure. The testing fluid was water with density $\rho_w = 1000 \, \text{kg/m}^3$ and kinetic viscosity $\mu = 1.01 \times 10^{-3} \, \text{Pa s}$ at the room temperature state. In order to obtain stable readings,
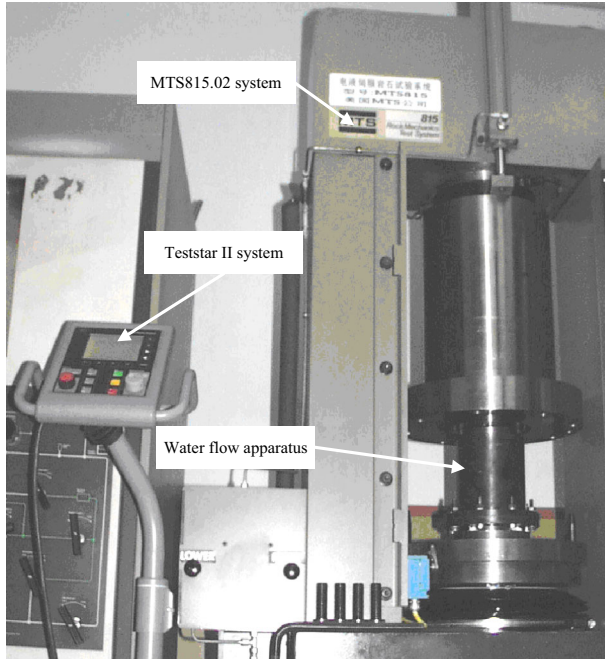
Fig. 5 MTS815.02 system and a self-made water flow apparatus
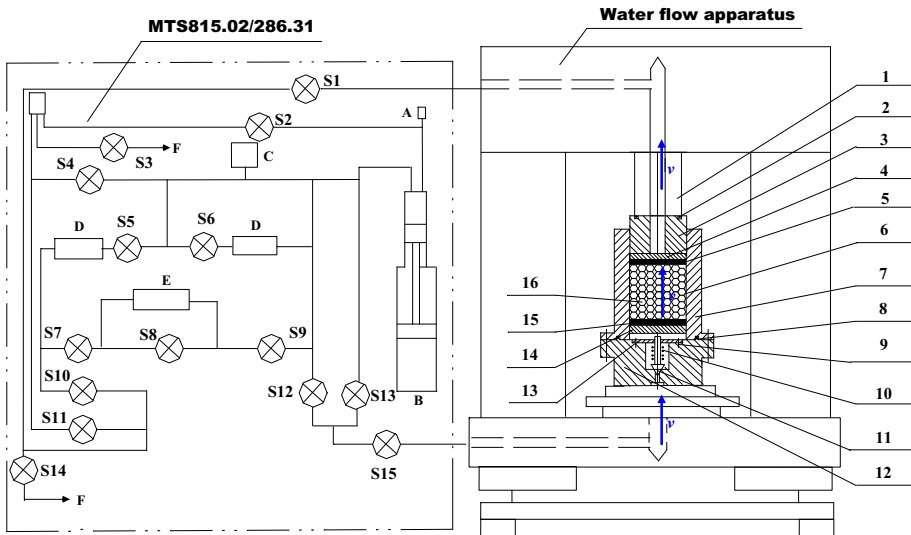

Fig. 6 Testing system of permeability of crushed rocks under variable grains diameter and axial displacement. *A*—pressure sensor, *B*—load controller, *C*—relief valve, *D*—regulator, *E*—pressure difference sensor, *F*—drainage, *S1–S15*—switch, *1*—loading platen, *2,8*—O-shaped rubber seal rings, *3*—piston, *4,14*—porous plate, *5,15*—felt filtration pad, *6*—epoxy resin separation layer, *7*—cylinder tube, *9*—mechanical bolt, *10*—mechanical spring, *11*—valve core, *12*—valve chest, *13*—base plate, *16*—crushed mudstone sample
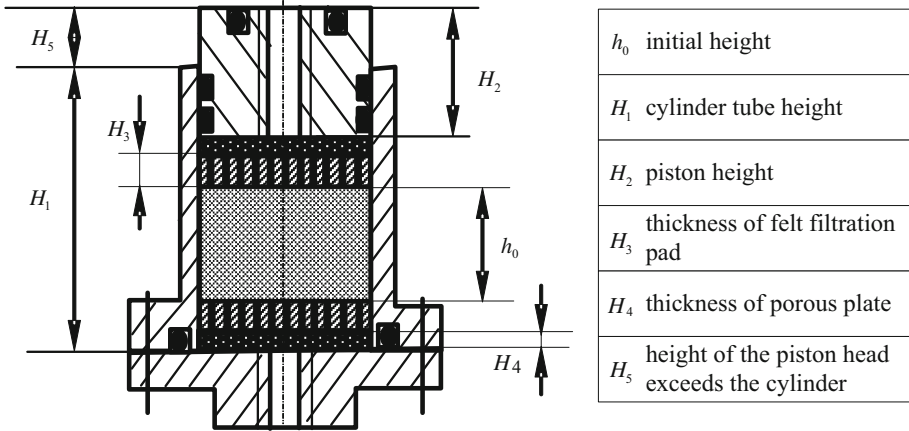
Fig. 7 Sketch calculating the height of the crushed mudstones

water flow measurements were carried out after the axial load was maintained at fixed level, i.e., the load change and water flow, respectively, belong to two different test stages. The five groups of crushed mudstone samples were tested one by one.

The test steps are as follows:

Step 1. Calculate the initial height of the rock sample before loading.

First, weigh the crushed rock sample with a mass m of 1800 g, place the rock into the cylinder tank, and then install the piston to preliminarily compact the sample. As shown in Fig. 7, according to the cylinder tube height H_1 (180 mm), the piston height H_2 (110 mm), the thickness of the felt filtration pad H_3 (9 mm), the thickness of porous plate H_4 (2 mm), and H_5 is the height that the piston head exceeds the cylinder, we can calculate the initial height h_0 of the crushed rock sample in the cylinder tank $h_0 = H_1 - H_2 - 2H_3 - 2H_4 + H_5$.

Because H_1, H_2, H_3 and H_4 were determined when the seepage device was designed, we can calculate h_0 by H_5, $h_0 = 180 - 110 - 18 - 4 + H_5 = 48 + H_5$.

Step 2. Saturate rock sample.

Saturate the rock sample with a water injection using the MTS815.02 test system.

Step 3. Apply the axial load.

Apply the axial load to the sample, keeping it steady until step 4 is ending.

Step 4. Apply the water seepage to the sample.

The shifting velocity v_p of the pressure intensifier piston can be controlled by programming in the MPT software platform of the MTS815.02 system. In the Scheme, after the first stress level was loaded up and kept steady, an axial pore pressure control mode was applied in the experiments: to produce different piston velocities of 10, 20, 30 and 35 mm min^{-1} for axial displacements of 10, 15, 20, 25, 30, 35 and 40 mm.

In the test, the seepage velocity is set with four different levels, so we can obtain the corresponding four levels of pore pressure gradient when the seepage is stable. The curve between the seepage velocity and pore pressure gradient can be fitted to calculate the seepage property parameters of the rock (Miao et al. 2004, 2011; Ma et al. 2013, 2014). Figure 8 illustrates the entire experimental procedure, and each of the rock samples will be conducted for three times to keep the accuracy; the final result is the average value of the three times testing values.

The entire experimental process was conducted according to the requirements previously established by the Teststar II system. By using the menu of the main form, the system has
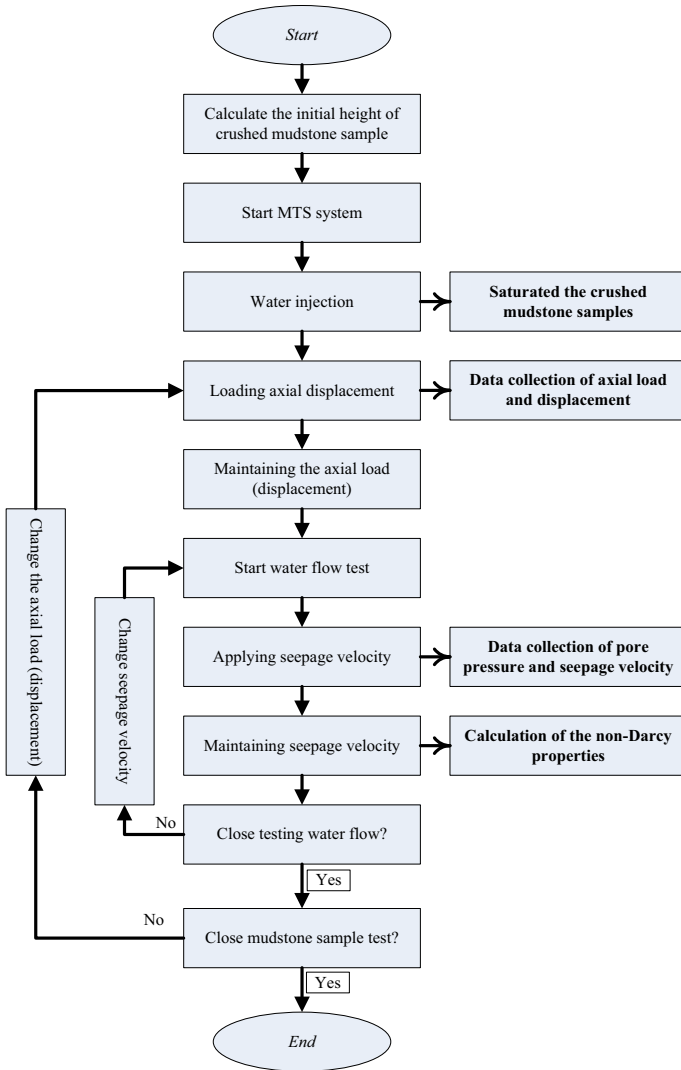
Fig. 8 Testing procedure of crushed mudstone

functions of distributing sensors, defining control models, setting boundaries, setting sensitive elements at zero automatically and selecting output signals. The system software included a GUI data interface, a software function generator, program designs and system tools. The Teststar II system was used to collect and process the test data.

4 Non-Darcy Flow Seepage Properties

4.1 Non-Darcy Approach

The porosity ϕ of each displacement level can be developed as follows

$$\phi = 1 - \frac{m}{\rho_s Q(h_0 - S)} \tag{1}$$

where m, ρ_s and h_0 are the mass, mass density and the initial height of the crushed mudstone sample, respectively, Q is the cross section area of the cylinder tube, and S is axial displacement.

The Forchheimer equation (Forchheimer 1914) can be used to model our investigation since it has proved to fit the water flow in crushed rocks well (Miao et al. 2004; Li et al. 2005; Miao et al. 2011; Liu et al. 2012; Ma et al. 2014). For a one-dimensional non-Darcy flow, the relationship between pressure and flow velocity can be expressed as

$$- \partial p / \partial z = \mu k^{-1} v + \rho_w \beta v^2 \tag{2}$$

where $\partial p / \partial z$ is the pore pressure gradient, p is the pore pressure, z is the vertical axis going through the center of the specimen, μ is the kinetic viscosity of the water, k is the permeability of the crushed mudstones, and v is average water flow velocity. ρ_w is the water density, and β is non-Darcy coefficient. When the value of β obtained from the experiment is close to zero, the flow satisfies the Darcy law.

The non-Darcy equation (Eq. 2) can be used to model the water flow in crushed rocks: For the crushed rocks, Reynolds number (Re) is defined as:

$$Re = \frac{\rho_w v d}{\mu \phi} \tag{3}$$

where d is the characteristic size, and for the non-consolidated crushed rocks, d is the average diameter of the grains, while for the consolidated crushed rocks, d is the average value of the capillary diameters; ϕ is porosity of the crushed rocks. The flow velocity v is controlled by keeping constant the displacement of the supercharger piston. The relationship between flow velocity v and supercharger piston velocity v_p can be defined as

$$v = v_p d_p^2 / d_r^2 \tag{4}$$

where d_p is the diameter of piston, and d_r is the diameter of sample (cylinder tube). In the test, the diameter of piston d_p is 55 mm, the diameter of sample d_r is 105 mm, so Eq. (4) can be wrote as

$$v = 55^2 / 105^2 v_p = 0.2744 v_p \tag{5}$$

4.2 Water Seepage Property Measurement Principle

The steady-flow method was selected to measure the impact of particle mixture on water flow in crushed mudstones. Specimen dimensions, water flux and seepage pressure must be measured to calculate the permeability k and non-Darcy coefficient β.

The first purpose of this test is to obtain the steady pore pressure corresponding to each flow velocity v. In the test, the upstream end of the mudstone specimen was connected to the pressure intensifier tank of the test system, which could automatically record the changing pore water pressure p over time t. p_b was assumed to be the steady value of p at the intake boundary. In our tests, the downstream end is connected with the atmosphere, resulting in a pore water pressure p_a equal to zero. The flow velocity is fixed and the flow in the mudstone specimen is steady if p is steady and the height of specimen is kept constant during seepage. Therefore, the pore pressure gradient is also steady.

Then, the steady pore pressure gradient is calculated. If all the parameters on the right side of Eq. (2) do not change with z, then the pore pressure gradient $\partial p / \partial z$ is a constant and can be determined by the pore pressure at the two ends of sample and then we can get

$$\partial p / \partial z = -(p_a - p_b) / L = -p_b / L = p / L \tag{6}$$

where L is the mudstone sample length. The one-dimensional seepage direction z is vertically upward, and if a steady flow dominates, then

$$p/L = \mu k^{-1} v + \rho_w \beta v^2 \tag{7}$$

The permeability k and non-Darcy coefficient β were calculated by the relationship between pressure gradient and fluid velocity curve (p–v curve). According to a group of flow velocity $v_1, \ldots, v_i, \ldots, v_n$ and the corresponding steady pressure gradients $p_1, \ldots, p_i, \ldots, p_n$, the values of non-Darcy seepage properties (permeability k and non-Darcy coefficient β) can be obtained by a second-order polynomial method at each particle mixture level,

$$\begin{cases} k = \dfrac{\mu\left[\left(\sum_{i=1}^n v_i^3\right)^2 - \sum_{i=1}^n v_i^2 \sum_{i=1}^n v_i^4\right]}{\sum_{i=1}^n p_i v_i^2 \sum_{i=1}^n v_i^3 - \sum_{i=1}^n p_i v_i \sum_{i=1}^n v_i^4} \\[4mm] \beta = \dfrac{\sum_{i=1}^n p_i v_i \sum_{i=1}^n v_i^3 - \sum_{i=1}^n p_i v_i^2 \sum_{i=1}^n v_i^2}{\rho_w\left[\left(\sum_{i=1}^n v_i^3\right)^2 - \sum_{i=1}^n v_i^2 \sum_{i=1}^n v_i^4\right]} \end{cases} \tag{8}$$

where n is the total flow times of each sample, $1 \leq i \leq n$, in the test, $n = 4$.

5 Test Results and Discussion

The non-Darcy seepage properties of crushed mudstone samples of particle sizes a (2.5–5 mm), b (5–10 mm), c (10–15 mm) and d (15–20 mm) as weight ratio 1:1:1:1, 3:1:1:1, 1:3:1:1, 1:1:3:1 and 1:1:1:3 are tested under variable axial displacement (10, 15, 20, 25, 30, 35 and 40 mm), respectively. According to Eqs. (1) and (8), the porosity ϕ and non-Darcy seepage properties (permeability k and non-Darcy coefficient β) of each displacement level can be calculated as shown in Table 2.

5.1 Steady-State Measurement

As shown in Fig. 9, about 20–25 s is required to attain to a seepage steady state for each flow. At each axial displacement level, the stability of the water pore pressure corresponding to the first velocity is comparatively weak. This is probably due to that the crushed mudstone sample had just undergone the earlier axial deformation and its pore structure was being adjusted locally.

5.2 Non-Darcy Seepage Flow

5.2.1 Re Calculation

A study shows that the upper limit of Re suitable for Darcy law is 5 and that for different porous media, this limit is slightly different (Kong 2010). We can calculate the Re according to Eq. (3) to prove the non-Darcy equation (Eq. 2) can be used to model the water flow in crushed mudstones. As shown in Table 2, the porosity ϕ of each displacement level was calculated based on Eq. (1), $\phi_{min} = 0.0958$, $\phi_{max} = 0.3637$. In the test, $v_{min} = 3.13 \times 10^{-2}$ mm/s, $v_{max} = 1.09 \times 10^{-1}$ mm/s. Taking $d = 2.5 - 20$ mm, $\phi = [0.0958, 0.3637]$, $\rho_w = 1000$ kg/m^3 and $\mu = 1.01 \times 10^{-3}$ Pa s into Eq. (3), we have

Table 2 Non-Darcy seepage properties under variable porosity

No.	Properties	Axial displacement (mm)						
		10	15	20	25	30	35	40
1	ϕ	0.3128	0.2842	0.2531	0.2191	0.1819	0.141	0.0958
	k (μm^2)	15.267	12.568	10.161	11.193	8.622	7.318	5.231
	β (mm^{-1})	4.864	6.796	9.801	8.296	13.002	17.229	30.709
2	ϕ	0.3182	0.2901	0.2595	0.2261	0.1896	0.1495	0.1052
	k (μm^2)	24.764	20.455	16.601	14.498	11.232	12.894	9.303
	β (mm^{-1})	2.117	2.941	4.212	5.316	8.249	6.504	11.41
3	ϕ	0.3289	0.3016	0.272	0.2398	0.2046	0.166	0.1235
	k (μm^2)	30.312	25.196	20.613	22.350	17.507	17.037	12.503
	β (mm^{-1})	1.495	2.054	2.905	2.525	3.846	4.028	6.861
4	ϕ	0.3392	0.3128	0.2842	0.2531	0.2191	0.1819	0.141
	k (μm^2)	25.231	20.15	20.964	16.582	14.623	11.782	8.42
	β (mm^{-1})	2.051	3.018	2.819	4.221	5.241	7.595	13.538
5	ϕ	0.3637	0.3392	0.3128	0.2842	0.2531	0.2191	0.1819
	k (μm^2)	31.333	26.550	22.204	26.226	21.201	23.763	18.311
	β (mm^{-1})	1.412	1.878	2.555	1.918	2.765	2.272	3.562

$$\begin{cases} Re_{min} = \frac{\rho_w v_{min} d_{min}}{\mu \phi_{max}} = 0.213 \\ Re_{max} = \frac{\rho_w v_{max} d_{max}}{\mu \phi_{min}} = 22.53 \end{cases} \tag{9}$$

So, $Re = [0.213, 22.53]$, $Re_{min} = 0.213$, $Re_{max} = 22.53$. It is possible that Re is greater than 5 and non-Darcy flow follows (Kong 2010). This means non-Darcy flow can be observed in specific cases.

5.2.2 Pore Pressure Gradient-Flow Velocity Curves

Figures 10 and 11 show that the water flow properties of crushed mudstones are found to be strongly influenced by axial displacement and particle size; in general, $\partial p / \partial z - v$ curves belong to quadratic relation, which shows the quadratic model of non-Darcy seepage, i.e., Forchheimer equation, Eq. (2) can fit the water flow in crushed mudstones under variable axial displacement and particle size.

5.3 Porosity Evolution During Compaction

According to Table 2, the porosity ϕ of each displacement level can be obtained in Fig. 12. The results in Fig. 12 show that: in general, the porosity of crushed mudstones is strongly influenced by compaction (axial displacement) and particle mixture. To same particle size weight ratio sample, the porosity decreases with the increase in axial displacement, and void in crushed sample becomes less during compaction. To same compaction (axial displacement) level, the porosity increases with the increase in bigger particle size, the weight ratio 1:1:1:3 shows maximum; this is because the volume of void in bigger particle size sample is greater than that in little size. The weight ratio 1:1:1:1 shows minimum, because the little particle
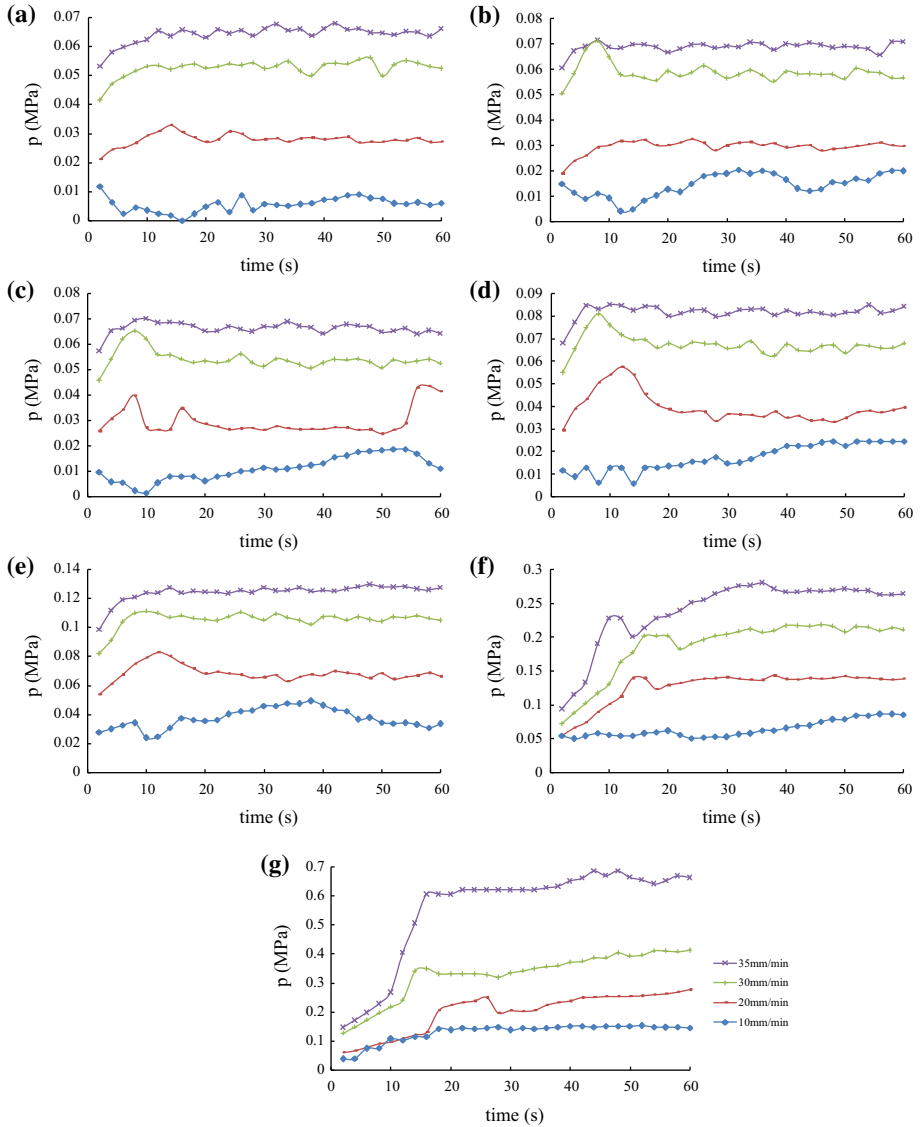
Fig. 9 Sample 1:1:1:1 pore pressures–time at variable axial displacement. **a** 10 mm, **b** 15 mm, **c** 20 mm, **d** 25 mm, **e** 30 mm, **f** 35 mm, g 40 mm

size rocks are filled in the void of bigger sizes; the particles to each other in the sample are closer than those in other samples. As shown in Fig. 13, the porosity change rate of sample particle size 1:1:1:1 shows greater when compared with that of other samples, which indicate the particle mixture (initial porosity) plays an important role in compaction, e.g., at the axial displacement 40 mm compared with 10 mm, the porosity change rate to each sample show as: sample 1:1:1:1 (0.69), 3:1:1:1 (0.67), 1:3:1:1 (0.62), 1:1:3:1 (0.58) and 1:1:1:3 (0.50), respectively, so compaction to smaller particle size mudstone sample have a bigger sensibility than that to larger one.

Fig. 10 Relation of pore
pressure gradient with flow
velocity of sample 1:1:1:1
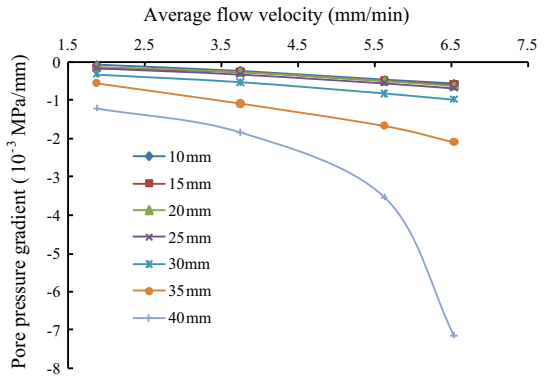
Fig. 11 Relation of pore
pressure gradient with flow
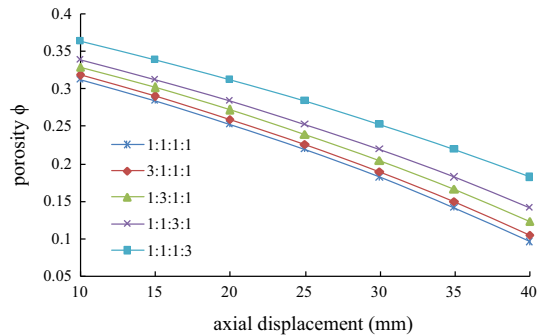velocity at axial displacement
10 mm
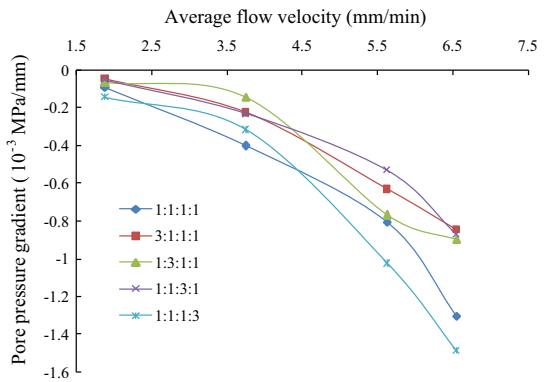
Fig. 12 Porosity of each axial
displacement level

5.4 Particle Crushing

Using the screening test sieve machine in laboratory (Fig. 3), the particle size weight of the
tested mudstones, before and after test (seepage and compaction), is determined in Table 3.
From the typical particle size weight distribution shown in Table 3 and weight change curves
after test shown in Fig. 14, the results show that compared to the original size weight distri-
bution, the size (15–20 mm) after test is decreased for each sample. The decreased position
indicates that during the compaction, some larger particles (15–20 mm) were crushed. The
particle weight change for mid-size (5–10 mm and 10–15 mm) after compaction is almost

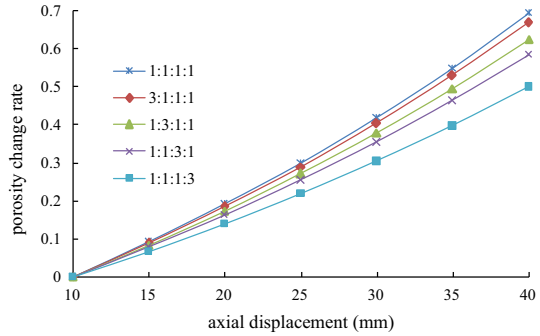**Fig. 13** Porosity change rate of each axial displacement level

Table 3 Particle size weight before and after test (seepage and compaction)

| No.	Weight to each particle size (g)								Weight change (g)	
	2.5–5 mm		5–10 mm		10–15 mm		15–20 mm		0–2.5 mm (increase)	Wight lost
	Before	After	Before	After	Before	After	Before	After		
1	450	462.1	450	448.6	450	451.3	450	410	16.8	11.2
2	900	885.4	300	309.5	300	298.4	300	278.5	12.3	15.9
3	300	313.4	900	885.2	300	297.1	300	278.4	11.4	14.5
4	300	309.2	300	301.3	900	891.2	300	272	13.5	12.8
5	300	319.2	300	302.5	300	294.1	900	857.6	17.2	9.4

Fig. 14 Weight change curves after test (+ means increased, − means lost)
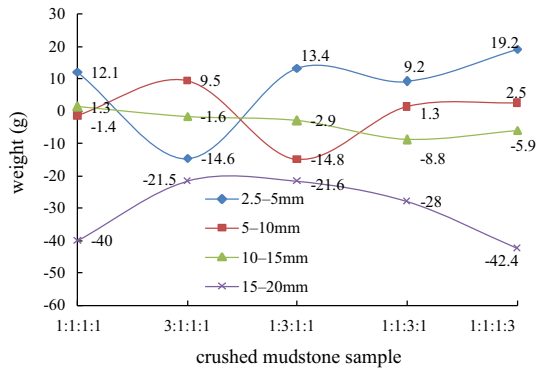
same, which means that the effects of mid-size on the amounts of particle crushing, during the compaction, are very small. The weight of size (2.5–5 mm) after compaction to each samples is almost increased (except sample 2), and during the compaction, some larger particles (15–20 mm) were crushed into small sizes, which causes the increase in the weight of size (2.5–5 mm).

Due to the compaction, some larger particles were crushed into small sizes, which include size 0–2.5 mm. There is some weight lost because of the effect of water seepage, so mud was washed away. Figure 15 shows weight of the size (0–2.5 mm) and lost to each sample; weight of the size (0–2.5 mm) for samples particle size 1:1:1:1 and 1:1:1:3 shows biggest, which is main because larger particles can be crushed into small sizes (0–2.5 mm) easily;

Fig. 15 Weight of the size (2.5–5 mm) and lost after test
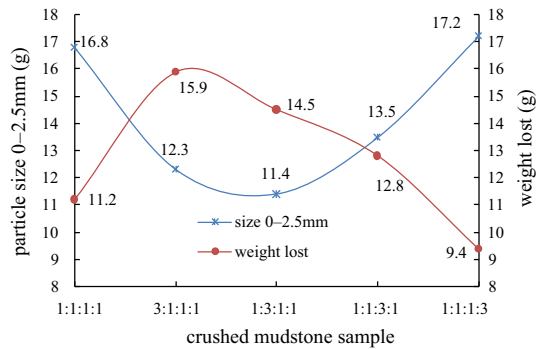
the weight lost for samples particle size 1:1:1:1 and 1:1:1:3 shows lowest, which means that mud in larger particles was difficult to be washed away. Anymore, due to the sample particle size 3:1:1:1 containing more small size (0–2.5 mm) than other samples, mud in the sample was easy to be washed away.

5.5 Non-Darcy Seepage Properties

Based on Table 2, the curves of k and β changing with porosity ϕ for the five particle mixture sizes are presented in Fig. 16.

From Fig. 16, it is seen that during the axial compression, the permeability k decreases while the non-Darcy coefficient β increases with the decrease in porosity ϕ except some local fluctuations. However, in the course of loading, due to the crushing of edges and corners and the adjustment of the structure, the pore channels become more uncertain; as a result, both the k–ϕ and β–ϕ curves display some local fluctuation (such as Fig. 16e when porosity $\phi \in (0.21, \ 0.33)$, k and β occur fluctuation).

In order to compare the seepage properties of these five particle mixture sizes of crushed mudstones, curves of the permeability k and non-Darcy coefficient β varying with porosity ϕ are shown in Fig. 17.

In general, the larger the particle size sample, the higher the permeability, which shows that the pores and cracks in mudstones of larger size can be easily narrowed. For example, as shown in Fig. 16e, the permeability k of weight ratio 1:1:1:3 shows one order of magnitude greater than that of weight ratio 1:1:1:1 in Fig. 16a, while the non-Darcy coefficient β is one to two orders smaller. As shown in Fig. 16a, the permeability k of uniform distribution of mixture size (weight ratio 1:1:1:1) meets minimum when compared with that of other samples, this is main because the smaller particle size as the calking of the larger ones, the porosity of uniform distribution is less than others, so its permeability to be a minimum.

Pore and crack absence and narrowing due to compaction (axial displacement increase) certainly contribute mostly to the decrease in permeability k and increase in coefficient β. An exception is that the abnormal climb in permeability k display some local fluctuation, which is probably due to the accumulation of gravel particle in widened fractures and accelerated flow. At the critical axial displacement (15 and 20 mm), isolated pores and cracks are able to complete the transformation from self-expansion to interconnection, which rapidly increases permeability. In addition, compared with smaller sizes, bigger one seems to have a less distinct critical axial displacement. A rational explanation is that bigger particle size specimens own many more effective pores and cracks that decrease permeability before uploading axial pressure (displacement). In a word, the seepage properties of crushed mudstones are not only
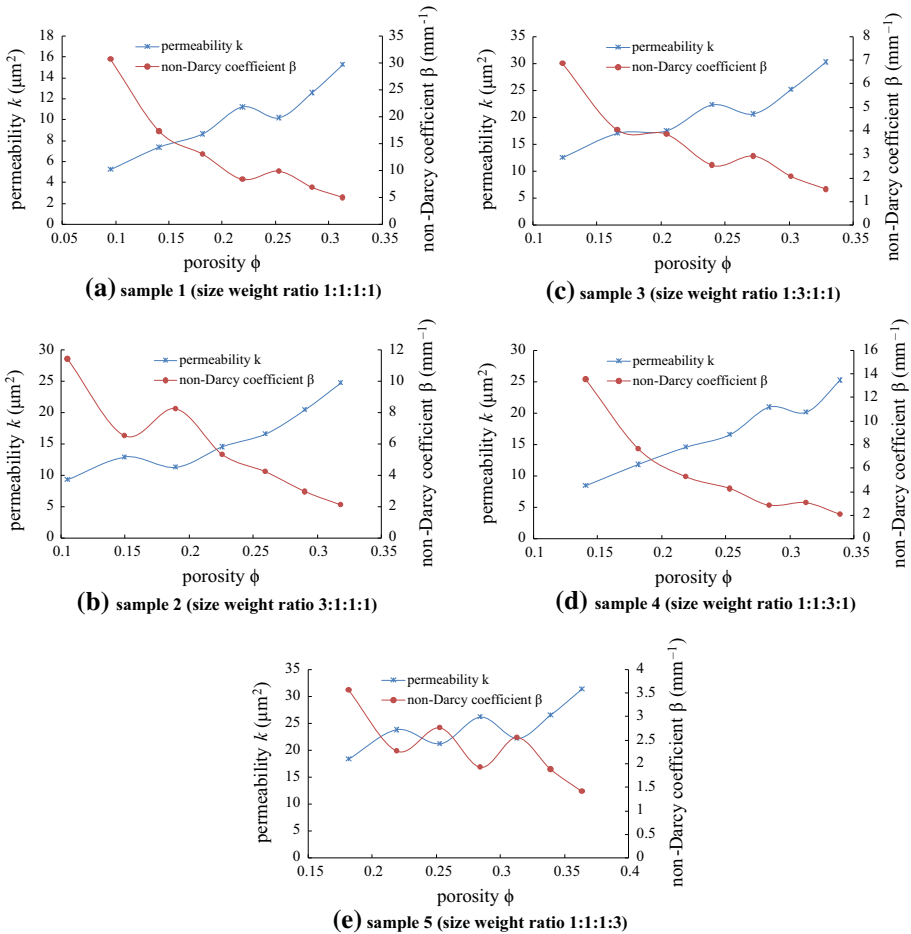
**Fig. 16** Non-Darcy seepage properties for five mixture sizes at various porosities

related to loading levels but also related to particle mixture, style of arrangement and initial pore structure.

6 Conclusions

An experiment based on a self-designed water flow apparatus, the MTS 815.02 system and a non-Darcy testing method were performed to investigate the effect of particle size mixture on seepage properties and compaction behavior of crushed mudstones. The following conclusions can be drawn.

- For steady-state measurement, about 20–25 s is required to attain a seepage steady state for each flow.
- The Re calculation, the pore pressure gradient and flow velocity curves of particle mixture show that the relation of pore pressure gradient and flow velocity can be fitted by the

Fig. 17 Comparison of non-Darcy seepage properties for five mixture sizes

(a) k–ϕ cures

(b) β–ϕ cures
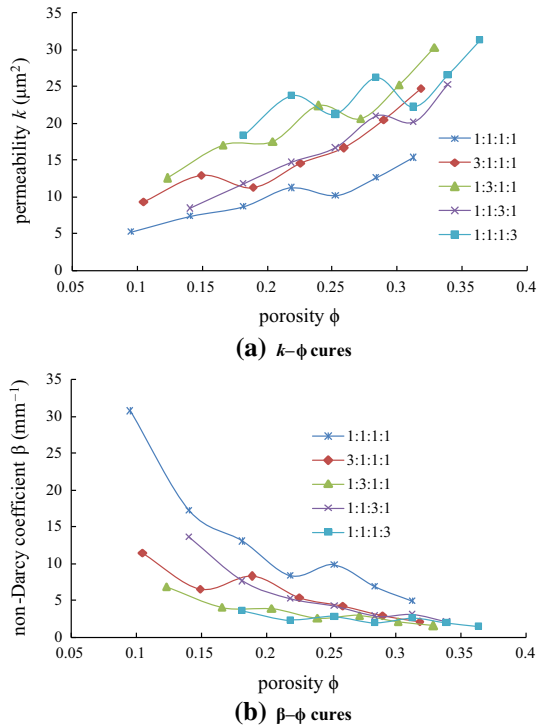
Forchheimer equation, Eq. (2), i.e., the water seepage flow in crushed mudstones is a non-Darcy flow.

- In general, the porosity of crushed mudstones is strongly influenced by compaction (axial displacement) and particle mixture. The porosity decreases with the increase in axial displacement and decrease in bigger particle size, respectively.
- During the compaction, some larger particles (15–20 mm) were crushed, which is a main reason to cause size 0–2.5 mm. Muds washed away are the main reason for weight lost in mudstone samples due to the effect of water seepage.
- Non-Darcy seepage properties (k and β) of crushed mudstones were strongly influenced by mixture sizes and compaction, in general, during the axial compression, the permeability k decreases while the non-Darcy coefficient β increases with the decreasing in porosity ϕ.
- The fluctuations of k–ϕ and β–ϕ curves show that the lager the particle size, the more the fluctuation displayed in the curves. The permeability k of minimum size shows one order of magnitude less than that for largest one.
- The seepage properties of crushed mudstones are not only related to compaction levels, mixture sizes, but also related to the style of arrangement.

References

Aydin, A., Borja, R.I., Eichhubl, P.: Geological and mathematical framework for failure modes in granular rock. J. Struct. Geol. **28**(1), 83–98 (2006)

Bai, H.B., Ma, D., Chen, Z.Q.: Mechanical behavior of groundwater seepage in Karst collapse pillars. Eng. Geol. **164**, 101–106 (2013)

Blodgett, S., Kuipers, J.R.: Underground Hard-Rock Mining: Subsidence and Hydrologic Environmental Impacts. Centre of Science in Public Participation, Bozeman (2002)

Blotz, L.R., Benson, C.H., Boutwell, G.P.: Estimating optimum water content and maximum dry unit weight for compacted clays. J. Geotech. Geoenviron. Eng. ASCE **124**(9), 907–912 (1998)

Casini, F., Viggiani, G.M.B.: Experimental investigation of the evolution of grading of an artificial material with crushable grains under different loading conditions. In: Proceedings of the 5th International Symposium on Deformation Characteristics of Geomaterials, Seoul, Korea, pp. 957–964 (2011)

Casini, F., Viggiani, G.M.B., Springman, S.M.: Breakage of an artificial crushable material under loading. Granul. Matter **15**(5), 661–673 (2013)

Chen, Z.Q., Miao, X.X., Mao, X.B.: Stability of Forcheimer's non-Darcy flow and probability of water inrush in coal mine. In: Proceedings of the 5th International Symposium on Mining Science and Technology, pp. 513–516 (2004)

Cho, G.-C., Dodds, J., Santamarina, J.C.: Particle shape effects on packing density, stiffness, and strength: natural and crushed sands. J. Geotech. Geoenviron. Eng. ASCE **132**(5), 591–602 (2006)

Coop, M.R., Sorensen, K.K., Freitas, T.B., Georgoutsos, G.: Particle breakage during shearing of a carbonate sand. Geotechnique **54**(3), 157–163 (2004)

Ding, H.D., Miao, X.X., Ju, F., Wang, X.L., Wang, Q.C.: Strata behavior investigation for high-intensity mining in the water-rich coal seam. Int. J. Min. Sci. Technol. **24**(3), 299–304 (2014)

Engelhardt, I., Finsterle, S.: Thermal-hydraulic experiments with bentonite/crushed rock mixtures and estimation of effective parameters by inverse modeling. Appl. Clay Sci. **23**(1–4), 111–120 (2003)

Forchheimer, P.: Hydrolik. Teubner, Leipzig (1914)

Fredlund, D.G., Morgenstern, N.R., Widger, R.A.: The shear strength of unsaturated soils. Can. Geotech. J. **15**(3), 313–321 (1978)

Hamdani, I.H.: Optimum moisture content for compacting soils one-point method. J. Irrig. Drain. Eng. **109**(2), 232–237 (1983)

Hardin, B.O.: Crushing of soil particles. J. Geotech. Eng., ASCE **111**(10), 1177–1192 (1985)

Huang, X.W., Tang, P., Miao, X.X., Chen, Z.Q.: Testing study on seepage properties of crushed sandstone. Rock Soil Mech. **26**(9), 1385–1388 (2005)

Jamei, M., Guiras, H., Chtourou, Y., Kallel, A., Romero, E., Georgopoulos, I.: Water retention properties of perlite as a material with crushable soft particles. Eng. Geol. **122**(3–4), 261–271 (2011)

Johnsen, Ø., Chevalier, C., Lindner, A., Toussaint, R., Clément, E., Måløy, K.J., Flekkøy, E.G., Schmittbuhl, J.: Decompaction and fluidization of a saturated and confined granular medium by injection of a viscous liquid or a gas. Phys. Rev. E Am. Phys. Soc. **78**, 051302 (2008)

Johnsen, Ø., Toussaint, R., Måløy, K.J., Flekkøy, E.G., Schmittbuhl, J.: Coupled air/granular flow in a linear Hele-Shaw cell. Phys. Rev. E Am. Phys. Soc. **77**, 011301 (2007)

Kogure, K.: Experimental study on permeability of crushed rock. Mem. Def. Acad. Jpn. **16**(4), 149–154 (1976)

Kong, X.Y.: Advanced Mechanics of Fluid in Porous Media, 2nd edn. Press of University of Science and Technology of China, Hefei (2010)

Lade, P.V., Yamamuro, J.A., Bopp, P.A.: Significance of particle crushing in granular materials. J. Geotech. Eng. ASCE **122**(4), 309–316 (1996)

Legrand, J.: Revisited analysis of pressure drop in flow through crushed rocks. J. Hydraul. Eng. **128**(11), 1027–1031 (2002)

Li, S.C., Miao, X.X., Chen, Z.Q.: Nonlinear dynamic analysis on non-Darcy seepage in over-broken rock mass. J. China Coal Soc. **30**(5), 557–561 (2005)

Liu, W.Q., Fei, X.D., Fang, J.N.: Rules for confidence intervals of permeability coefficients for water flow in over-broken rock mass. Int. J. Min. Sci. Technol. **22**, 29–33 (2012)

Liu, W.Q., Miao, X.X., Chen, Z.Q.: A testing method for determining the permeability of overbroken rock. Chin. J. Exp. Mech. **18**, 56–61 (2003)

Lobo-Guerrero, S., Vallejo, L.E.: Discrete element method evaluation of granular crushing under direct shear test conditions. J. Geotech. Geoenviron. Eng. ASCE **131**(10), 1295–1300 (2005)

Ma, D., Miao, X.X., Chen, Z.Q., Mao, X.B.: Experimental investigation of seepage properties of fractured rocks under different confining pressures. Rock Mech. Rock Eng. **46**, 1135–1144 (2013)

Ma, D., Miao, X.X., Jiang, G.H., Bai, H.B., Chen, Z.Q.: An experimental investigation of permeability measurement of water flow in crushed rocks. Transp. Porous Media **105**, 571–595 (2014)

Ma, D., Bai, H.B., Wang, Y.M.: Mechanical behavior of a coal seam penetrated by a karst collapse pillar: mining induced groundwater inrush risk. Nat. Hazards. **75**, 2137–2151 (2015)

Ma, Z.G.: Studies on Characteristics of Water Seepage in Crushed Rock Mass of Gob. China University of Mining and Technology, Xuzhou (2003)

Miao, X.X., Li, S.C., Chen, Z.Q., Liu, W.Q.: Experimental study of seepage properties of broken sandstone under different porosities. Transp. Porous Media **86**, 805–814 (2011)

Miao, X.X., Liu, W.Q., Chen, Z.Q.: Seepage Theory of Mining Strata. Science Press, Beijing (2004)

MTS System Corporation: Teststar Materials Testing Workstation Installation Reference Manual (1993)

Niebling, M., Toussaint, R., Flekkøy, E.G., Måløy, K.J.: Dynamic aero fracture of dense granular packings. Phys. Rev. E Am. Phys. Soc. **86**, 061315 (2012)

Pappas, D.M., Mark, C.: Behavior of simulated longwall gob material. Report of investigations, US Bureau of Mines (1993)

Peng, S.S.: Longwall Mining, 2nd edn. Society for Mining Metallurgy, and Exploration, Littleton (2006)

Pradip, K.G.N., Venkataraman, P.: Non-Darcy converging flow through coarse granular media. J. Inst. Eng. (India) Civ. Eng. Div. **76**, 6–11 (1995)

Rong, H.R., Bai, H.B.: Pore structure characteristics of the relative water-resisting layer on the top of the ordovician in longgu coal mine. Int. J. Min. Sci. Technol. **24**(5), 657–661 (2014)

Shi, L.Q., Qiu, M., Wei, W.X., Xu, D.J., Han, J.: Water inrush evaluation of coal seam floor by integrating the water inrush coefficient and the information of water abundance. Int. J. Min. Sci. Technol. **24**(5), 677–681 (2014)

Singh, M.M.: Mine subsidence. In: Hartman, H.L. (eds.) SME Mining Engineers Handbook, pp. 938–71 (1992)

Wang, J.-J., Zhu, J.-G., Chiu, C.F., Zhang, H.: Experimental study on fracture toughness and tensile strength of a clay. Eng. Geol. **94**(1–2), 65–75 (2007)

Wang, J.-J., Zhang, H.-P., Zhang, L., Liang, Y.: Experimental study on heterogeneous slope responses to drawdown. Eng. Geol. **147–148**, 52–56 (2012)

Wang, J.-J., Zhang, H.-P., Zhang, L., Liang, Y.: Experimental study on self-healing of crack in clay seepage barrier. Eng. Geol. **159**, 31–35 (2013a)

Wang, J.-J., Zhao, D., Liang, Y., Wen, H.-B.: Angle of repose of landslide debris deposits induced by 2008 Sichuan Earthquake. Eng. Geol. **156**, 103–110 (2013b)

Wang, J.-J., Zhang, H.-P., Tang, S.-C., Liang, Y.: Effects of particle size distribution on shear strength of accumulation soil. J. Geotech. Geoenviron. Eng. ASCE **139**(11), 1994–1997 (2013c)

Wang, J.J., Zhang, H.P., Deng, D.P., Liu, M.W.: Effects of mudstone particle content on compaction behavior and particle crushing of a crushed sandstone-mudstone particle mixture. Eng. Geol. **167**, 1–5 (2013d)

Wu, D., Hu, Y., Fan, X.: Visual simulation for granular rocks crush in virtual environment based on fractal geometry. Simul. Model. Pract. Theory **17**(7), 1254–1266 (2009)

Xiaojihan Geological and Mineral Resource Exploration (XGMRE): Northern Shaanxi Jurassic Coal Area. Shaanxi Huadian Yuheng Coal Industry Co., Ltd, Shaanxi, China (2009)

Yan, Z.-L., Wang, J.-J., Chai, H.-J.: Influence of water level fluctuation on phreatic line in silty soil model slope. Eng. Geol. **113**(1–4), 90–98 (2010)

Zoback, M.D., Byerlee, J.D.: Note on the deformational behavior and permeability of crushed granite. Int. J. Rock Mech. Min. Sci. Geomech. Abstr. **13**(10), 291–294 (1976)